Dynamic microtubules regulate the local concentration of E-cadherin at cell-cell contacts

Samantha J. Stehbens[1,*], Andrew D. Paterson[1,2,*], Matthew S. Crampton[1], Annette M. Shewan[1], Charles Ferguson[1,3], Anna Akhmanova[4], Robert G. Parton[1,3] and Alpha S. Yap[1,‡]

[1]Division of Molecular Cell Biology, Institute for Molecular Bioscience, [2]School for Biomedical Science, and [3]Centre for Microscopy and Microanalysis, The University of Queensland, St Lucia, Brisbane, Queensland 4072, Australia
[4]MGC Department of Cell Biology and Genetics, Erasmus Medical Center, 3000 DR Rotterdam, The Netherlands

*These authors contributed equally to this work
‡Author for correspondence (e-mail: a.yap@imb.uq.edu.au)

Accepted 24 January 2006
Journal of Cell Science 119, 1801-1811 Published by The Company of Biologists 2006
doi:10.1242/jcs.02903

Summary

In contrast to the well-established relationship between cadherins and the actin cytoskeleton, the potential link between cadherins and microtubules (MTs) has been less extensively investigated. We now identify a pool of MTs that extend radially into cell-cell contacts and are inhibited by manoeuvres that block the dynamic activity of MT plus-ends (e.g. in the presence of low concentrations of nocodazole and following expression of a CLIP-170 mutant). Blocking dynamic MTs perturbed the ability of cells to concentrate and accumulate E-cadherin at cell-cell contacts, as assessed both by quantitative immunofluorescence microscopy and fluorescence recovery after photobleaching (FRAP) analysis, but did not affect either transport of E-cadherin to the plasma membrane or the amount of E-cadherin expressed at the cell surface. This indicated that dynamic MTs allow cells to concentrate E-cadherin at cell-cell contacts by regulating the regional distribution of E-cadherin once it reaches the cell surface. Importantly, dynamic MTs were necessary for myosin II to accumulate and be activated at cadherin adhesive contacts, a mechanism that supports the focal accumulation of E-cadherin. We propose that this population of MTs represents a novel form of cadherin-MT cooperation, where cadherin adhesions recruit dynamic MTs that, in turn, support the local concentration of cadherin molecules by regulating myosin II activity at cell-cell contacts.

Supplementary material available online at
http://jcs.biologists.org/cgi/content/full/119/9/1801/DC1

Key words: Cadherins, E-cadherin, Microtubules, Microtubule dynamics

Introduction

Classical cadherin adhesion molecules function as membrane-spanning macromolecular complexes. The binding properties of the cadherin ectodomains support surface adhesion and cell-cell recognition, whereas the cytoplasmic tails can interact with a range of proteins that couple cadherins to cell signalling pathways and to the cytoskeleton (Perez-Moreno et al., 2003). Importantly, cadherin-based cell-cell contacts are dynamic adhesive structures (Adams et al., 1998). Even the apparently commonplace observation that cadherins accumulate at cell-cell contacts reflects the ongoing interplay between local adhesive remodelling (Gumbiner, 2000), cytoskeletal association (Adams and Nelson, 1998; Shewan et al., 2005) and the trafficking and turnover of cadherins to and from the plasma membrane (Bryant and Stow, 2004). Such interplay, in turn, probably arises from dynamic interactions between cadherins and the cytoskeleton that are coordinated at the cell cortex by membrane-local cell signalling (Gumbiner, 2000; Perez-Moreno et al., 2003; Yap and Kovacs, 2003).

The microtubule (MT) cytoskeleton is a major determinant of cortical dynamics in a wide range of circumstances and MTs can interact with the cortices of animal cells in a variety of ways. One particularly striking interaction involves MT plus (+)-ends, which are commonly oriented towards the cell periphery (Akhmanova and Hoogenraad, 2005; Gundersen et al., 2004). Dynamic instability allows these (+)-ends to grow outwards and potentially explore peripheral structures (Howard and Hyman, 2003), including integrin-based focal adhesions (Small and Kaverina, 2003), as well as regions of the free cell surface (Gundersen et al., 2004). Moreover, there is increasing evidence that such interactions with MT(+)-ends affect cellular processes at the cortex, including the dynamics of integrin adhesion complexes and actin cytoskeletal activity (Rodriguez et al., 2003). MT(+)-ends might exert these effects by facilitating vesicular transport to the cell surface (Watanabe et al., 2005), as well as by delivering regulatory molecules to the cortex (Rodriguez et al., 2003).

In contrast to the well-established connection between cadherins and the actin cytoskeleton (Adams and Nelson, 1998), less is known about the potential relationship between cadherins and MTs. MTs are often identified in close proximity to cadherin contacts, where they are reported to organise in a variety of patterns that include running parallel to the lateral cell surface in polarised Madin-Darby canine kidney (MDCK) cells (Bacallao et al., 1989) and extending towards contacts in myoblasts (Mary et al., 2002). Furthermore, several recent studies have suggested molecular mechanisms that can link cadherins to MTs (Kaufmann et al., 1999). Thus, β-catenin is

reported to bind the MT-based motor dynein (Ligon et al., 2001), N-cadherin can form a complex with the KIF3 kinesin (Teng et al., 2005), and p120 catenin might interact both with conventional kinesin (Chen et al., 2003) and directly with MTs themselves (Yanagisawa et al., 2004). Without yet providing a comprehensive picture, these findings suggest the potential for cadherins to associate physically with MTs.

There is also emerging evidence for functional interaction between cadherins and MTs. Cell-cell contact in lung epithelial cells was reported to stabilise the dynamic behaviour of MT(+)-ends (Waterman-Storer et al., 2000), whereas N-cadherin adhesions could stabilise MT minus-ends in cytoplasts (Chausovsky et al., 2000). Therefore, cadherin-based adhesion can regulate MT dynamics. By contrast, MT integrity might also affect cadherins, as depolymerisation of MTs disrupted the morphology and organisation of E-cadherin-based contacts in thyroid monolayers (Waterman-Storer et al., 2000; Yap et al., 1995), whereas low concentrations of nocodazole that affect MT(+)-end dynamics perturbed the distribution of catenins at contacts between newt lung epithelial cells (Waterman-Storer et al., 2000). One way in which MTs might influence cell-cell contacts is through kinesin-based transport of cadherin-containing vesicles, which have been implicated in both the maintenance and reassembly of cell-cell adhesions (Chen et al., 2003; Mary et al., 2002).

Together, these disparate observations suggest the capacity for cadherin contacts to interact with the MT cytoskeleton, without yet providing a detailed understanding of what this could entail. We sought to pursue this possibility in this study. We identified a subpopulation of MTs that radiate into E-cadherin-based cell-cell contacts with their (+)-ends oriented towards cadherin adhesions. Importantly, the integrity of dynamic MTs was necessary both for cells to accumulate E-cadherin locally and to activate myosin II at cell-cell contacts, thus revealing a novel role for these MTs in controlling the regional distribution of cadherin once it is on the cell surface.

Results

E-cadherin adhesive contacts recruit a subpopulation of radially oriented MTs

We first used indirect immunofluorescence microscopy to compare the localisation of MTs and E-cadherin in MCF-7 cells, a well-differentiated mammary epithelial cell line that expresses E-cadherin. Many MTs extended from the

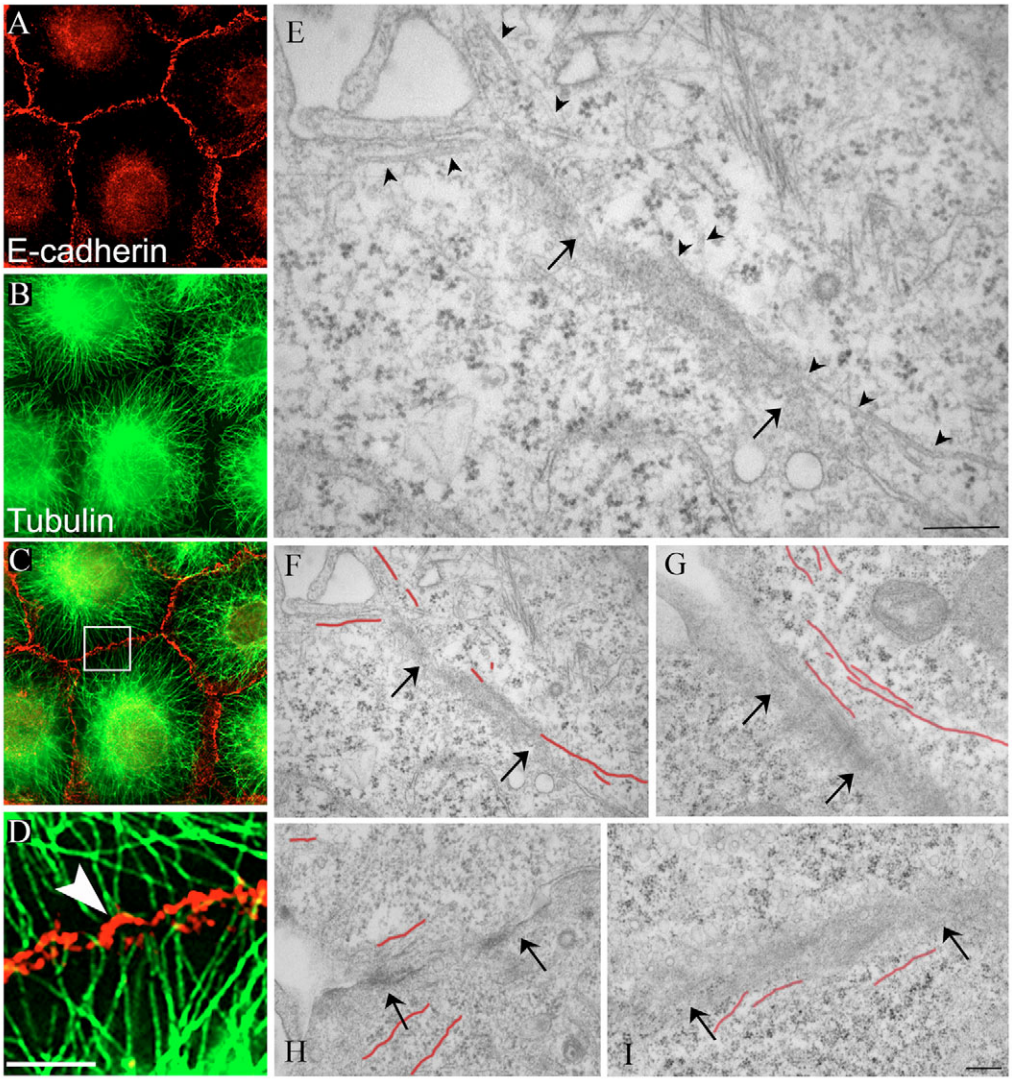

Fig. 1. A subpopulation of radially directed MTs extend into E-cadherin-based cell-cell contacts. MCF-7 cell monolayers were fixed at confluence and processed for epi-illumination immunofluorescence microscopy or electron microscopy. (A-D) Dual-label immunofluorescence imaging for E-cadherin (A) or β-tubulin (B). A subpopulation of MTs appeared to radiate from the perinuclear area into sites of cadherin-rich cell-cell contacts (C,D); D shows the magnified boxed region in panel C. Distal tips of these MTs often appeared to terminate in concentrations ('puncta') of E-cadherin staining (D, arrowhead). Bar, 5 μM in panel D. (E-I). Gallery of electron microscopic images of junctional areas in MCF-7 cells and in hE-CHO cells. MTs (arrowheads in E), recognised by their characteristic morphology, run close to the adherens junction (between arrows), in some cases entering the dense microfilament network underlying the junctional complex. Panels F-I show lower magnification views of junctional areas in which MTs have been traced by hand and coloured to facilitate their recognition (E and F show the same image, F with MTs traced). Bars, 200 nm (F-I same magnification).

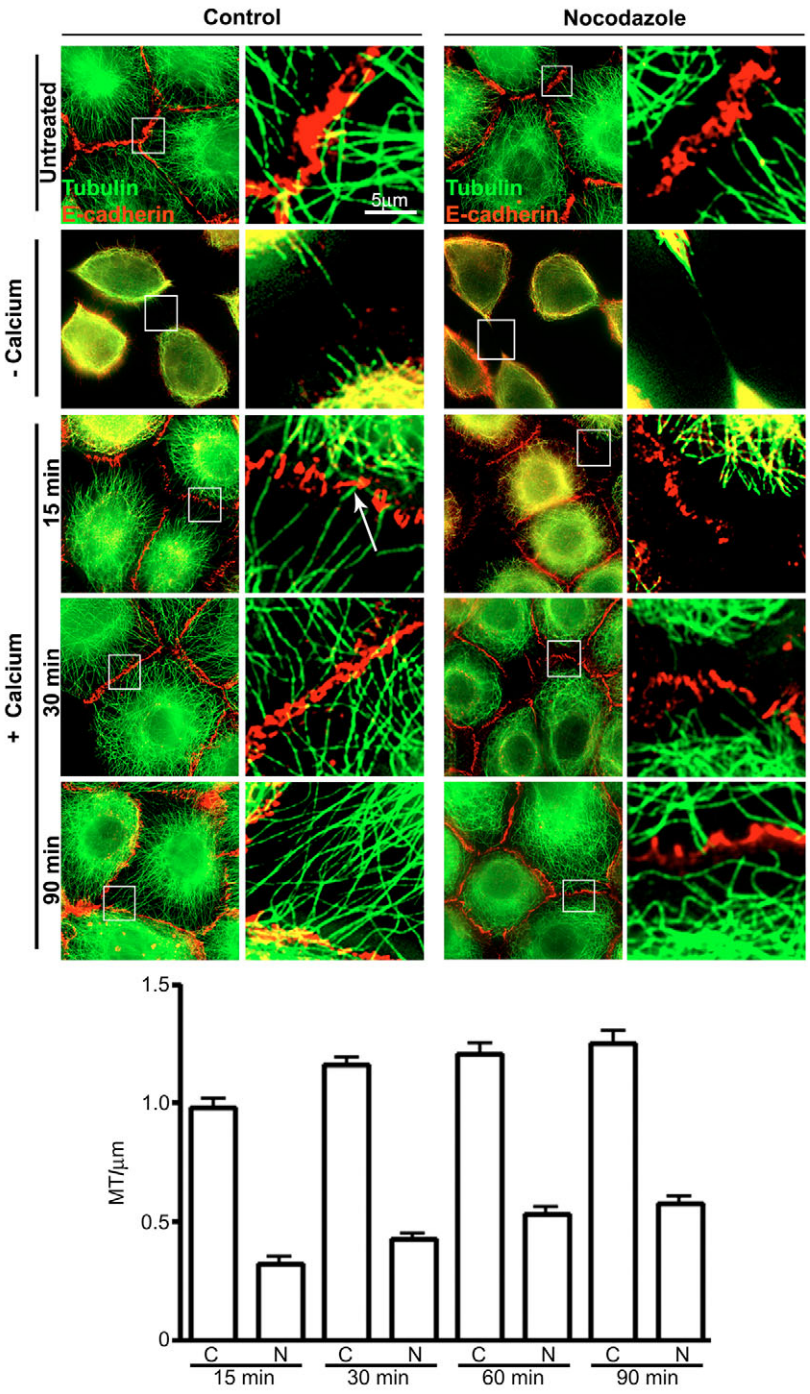

Fig. 2. Orientation of MTs as MCF-7 cultures reassemble cell-cell contacts. MCF-7 cells were fixed at confluence (untreated), immediately after incubation with 4 mM EGTA (–Calcium), or 15-90 minutes after replenishment of 5 mM extracellular Ca^{2+}. One set of cells were treated with nocodazole (100 nM, added 60 minutes prior to experiments and maintained in media for the duration of the experiments), whereas control cultures were grown in standard media supplemented with carrier (DMSO) alone. E-cadherin and β-tubulin were identified by dual-label epi-illumination immunofluorescence microscopy. The right-hand panel of each pair represent high-power details of the regions marked by the boxes. The density of MTs at contacts was quantitated by counting the number of MTs found within 3 μm of the E-cadherin-stained contacts. Data are means ± s.e.m., *n*=40, in control (C) or nocodazole (N)-treated cells. Prominent (or pioneer) MTs appeared to terminate in these cadherin accumulations (arrow), which became more numerous as cell contacts extended. Treatment of MCF-7 cells with low-dose nocodazole (100 nM) inhibited the formation of these pioneer MTs at reforming contacts.

perinuclear MT organisation centre (MTOC), but looped inwards before reaching the cell periphery. However, we also identified a radial pattern of MTs that extended further, apparently projecting into the E-cadherin-rich cell-cell contacts at varying angles (Fig. 1A-D). The tips of these MTs often appeared to terminate at local concentrations ('puncta') of E-cadherin. Radial MTs were consistently identified by staining for β-tubulin (Fig. 1), but were rarely found when stained for acetylated tubulin, which instead identified more centrally located MTs that seldom extended into contacts (Fig. S1, supplementary material). Similar subpopulations of radially oriented MTs were observed to terminate at cell-cell contacts in other epithelial cell lines (MDCK, NMuMG) and in Chinese hamster ovary (CHO) cells stably expressing human E-cadherin (hE-CHO cells; not shown). Furthermore, in electron micrographs of cell-cell contacts between MCF-7 cells and hE-CHO cells (Fig. 1E-I), MTs could be observed in close proximity to the adherens junctions.

A relationship between MTs and E-cadherin adhesions was also apparent as MCF-7 cells reassembled contacts following chelation of extracellular Ca^{2+} (Fig. 2). As cells rounded up after cell-cell contacts were broken by removal of Ca^{2+}, the outwardly directed networks of MTs were lost, with the exception of occasional MTs located in what appeared to be retraction fibres. After replacement of extracellular Ca^{2+}, cells spread to reassemble contacts with one another and E-cadherin rapidly reaccumulated in these nascent adhesions, commonly being found in distinct puncta at the cell-cell contacts. Strikingly, prominent MTs were found directed towards these nascent cadherin adhesions, often with their tips overlapping the puncta. Cadherin staining became more continuous, and these radially directed MTs became more numerous, as cell contacts extended (Fig. 2).

E-cadherin homophilic ligation is sufficient to recruit MTs into adhesive contacts

These observations suggested the possibility that cadherin adhesion might recruit MTs. To pursue this, we then asked whether cadherin homophilic ligation might be sufficient to recruit MTs into adhesive contacts (Fig. 3). For this purpose, we used a recombinant adhesive dimer consisting of the complete ectodomain of human E-cadherin fused to the Fc region of IgG (hE/Fc). This, and similar reagents, effectively support adhesion and stimulate cadherin signalling (Gavard et al., 2004; Kovacs et al., 2002a; Kovacs et al., 2002b). CHO cells were used in these experiments as they provide a

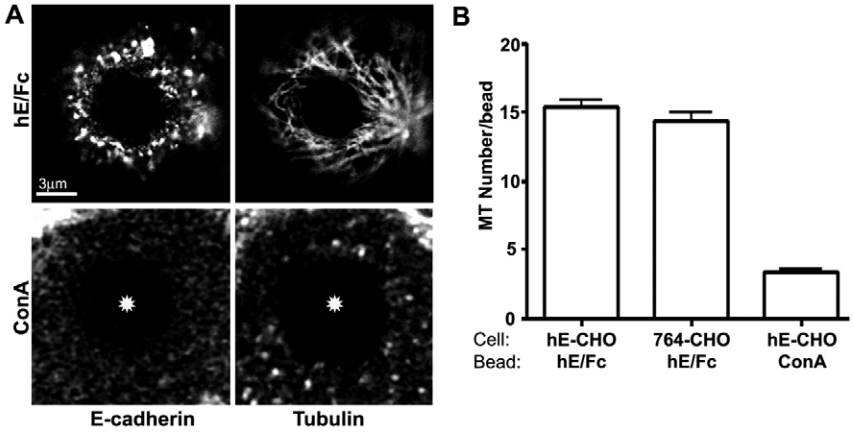

Fig. 3. E-Cadherin homophilic ligation is sufficient to recruit MTs into adhesion sites. CHO cells stably expressing full-length human E-cadherin (hE-CHO) and E-cadherin lacking the p120 binding site (764-CHO) were grown to 80% confluency on glass coverslips. Latex beads (6 mm diameter) coated with either hE/Fc or ConA were allowed to adhere to the dorsal surfaces of cells for 90 minutes. Samples were immunolabelled for E-cadherin and tubulin, and visualised by laser scanning confocal microscopy. (A) Adhesion of hE/Fc-coated beads, but not ConA beads (asterisks), was associated with the accumulation of E-cadherin around the beads and projection of MTs into the sites of adhesion. (B) MT recruitment was quantified by counting the number of individual MTs that extended into contacts made between hE/Fc or ConA-coated beads and cells expressing full-length E-cadherin (hE-CHO) or CHO cells expressing the hE-Cad 764AAA mutant (764-CHO). We included all MTs that appeared to come into contact with the beads. Data are means ± s.e.m. (n=30 beads) and are representative of three separate experiments.

cadherin-deficient background in which to express wild-type or mutant E-cadherin. Latex beads coated with hE/Fc efficiently adhered to the dorsal surfaces of hE-CHO cells, where they induced the accumulation of cellular E-cadherin around the adhesion site (Fig. 3A). Strikingly, MTs also extended into the adhesive sites between hE/Fc-beads and hE-CHO cells, as was also evident in three-dimensional (3D) projections from confocal stacks (not shown). By contrast, beads coated with the non-specific ligand concanavalin A (ConA) bound robustly to hE-CHO cells, but did not recruit MTs to any comparable extent, as quantitated by counting the number of MTs that extended into contacts (Fig. 3B). This indicated that cadherin homophilic ligation could exert an instructive effect to recruit MTs into adhesive contacts.

Taken together, these data suggest that cadherin adhesive contacts can recruit MTs through a process that responds to cadherin homophilic ligation. One potential molecule that might link MTs to classical cadherins is p120 catenin, which associates directly with the membrane-proximal region of the cadherin cytoplasmic domain and which can also bind, both directly and indirectly, to MTs (Chen et al., 2003; Franz and Ridley, 2004; Yanagisawa et al., 2004). We therefore tested whether a p120-uncoupled cadherin mutant could recruit MTs to adhesive sites, using CHO cells stably expressing hE-Cad 764AAA, which bears point mutations in the cytoplasmic tail that ablate interaction with p120 catenin (Goodwin et al., 2003; Thoreson et al., 2000). Adhesions between hE-Cad 764AAA CHO cells and hE/Fc beads recruited MTs as efficiently as the wild-type cadherin adhesions (Fig. 3B), suggesting that association with p120 catenin is not essential for E-cadherin to recruit MTs into homophilic adhesive contacts. Similar results were seen in A431D cells expressing either wild-type E-cadherin or hE-Cad 764AAA (not shown).

Radial MTs are oriented with (+)-ends directed towards cadherin contacts

MTs characteristically extend their plus (+)-ends towards cell peripheries. To test whether this pertained for the subpopulation of radially arrayed MTs that extended into cadherin contacts, we co-stained MCF-7 cells with an antibody that specifically recognises CLIP-170, a well-characterised MT(+)-end-binding protein (Komarova et al., 2002). In triple-labelled studies, CLIP-170 could be clearly identified in streaks at the tips of MTs that extended into E-cadherin-based cell-cell contacts (Fig. 4A,A'). Time-lapse imaging of cells expressing GFP-tagged CLIP-170 also revealed that streaks of CLIP-170 frequently moved into, and overlapped with, cadherin-based cell-cell contacts (not shown). This confirmed that the radially arrayed MTs were oriented with their (+)-ends directed towards cadherin contacts. It further suggested the possibility that this subpopulation of MTs might arise from the growth of MT(+)-ends into cadherin contacts.

To pursue this possibility, we then tested whether the dynamic integrity of MT(+)-ends was necessary to generate the radial MTs. We first treated cells with low concentrations of nocodazole that inhibit (+)-end turnover of tubulin monomers but do not disrupt the overall architecture of MTs (Jordan and Wilson, 1998; Perez et al., 1999). Confluent MCF-7 cell monolayers incubated with nocodazole (100 nM) for 60

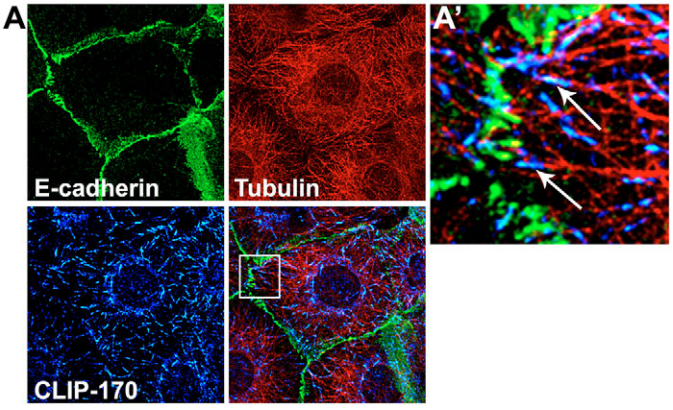

Fig. 4. Radial MTs extend with plus-ends directed towards cadherin contacts. MCF-7 cells were triple labelled for E-cadherin, tubulin and CLIP-170 and imaged by confocal microscopy (A). A magnified boxed region of the triple label overlay identified CLIP-170 at the tips of MTs that extended into E-cadherin-based cell-cell contacts (A', arrows).

minutes displayed fewer MTs at cadherin contacts than seen in vehicle-treated controls, although the overall integrity of the MT cytoskeleton was not grossly disrupted (Fig. 2). Moreover, when contacts were then manipulated by acute changes in extracellular Ca^{2+}, nocodazole dramatically reduced both the number of MTs found at reassembling contacts and the extent to which they projected towards the cadherin contacts (Fig. 2). Additionally, we found that radially arrayed MTs were much less apparent in cells expressing a CLIP-170 mutant lacking the C-terminus that associates with cortical binding partners (CLIP-170 Δ-Tail; Fig. S2, supplementary material). Rather than extending into contacts, MTs in cells transfected with CLIP-170 Δ-Tail formed thick filaments that looped through the cytoplasm, a pattern that characteristically arises when (+)-end dynamics are blocked by perturbing various MT(+)-end binding proteins (Ligon et al., 2003). Both nocodazole (Fig. S1, supplementary material) and CLIP-170 Δ-Tail (Fig. S2, supplementary material) increased the prominence of MTs that stained for acetylated tubulin; but, as with control cells (Fig. S1, supplementary material), the majority of these stabilised MTs did not extend into cadherin contacts. Taken together, these observations suggested strongly that the radial MTs that we have identified at cadherin contacts constitute a pool of dynamic MTs that extend into contacts through (+)-end growth.

Dynamic MTs support the local concentration of E-cadherin at cell-cell contacts

To investigate the potential impact of dynamic MTs on E-cadherin, we examined endogenous E-cadherin localisation in MCF-7 cell monolayers treated with low-dose nocodazole (100 nM; Fig. 5A). In contrast to the prominent continuous bands of E-cadherin that were readily evident between control cells, especially at the apices of contacts, nocodazole-treated cells showed staining that was less intense and more discontinuous. This suggested that blocking MT(+)-end dynamics might affect the ability of cells to concentrate E-cadherin at cell-cell contacts. To extend this, we then asked whether nocodazole also affected the ability of E-cadherin to accumulate in newly forming cell-cell contacts in the Ca^{2+} manipulation assays (Fig. 5B). Although E-cadherin did localise to nascent contacts in these experiments, the intensity of staining appeared reduced in nocodazole-treated cells compared with controls. Indeed, quantitation of fluorescence intensity revealed that nocodazole significantly reduced the amount of cadherin present at cell-cell contacts throughout the duration (60 minutes) of these experiments (Fig. 5B). Similarly, E-cadherin fluorescence intensity was reduced by >50% between cells expressing CLIP-170 Δ-Tail compared with contacts between control cells (Fig. 6). Taken together, these observations suggested that dynamic MTs were necessary for cells to concentrate E-cadherin at cell-cell contacts.

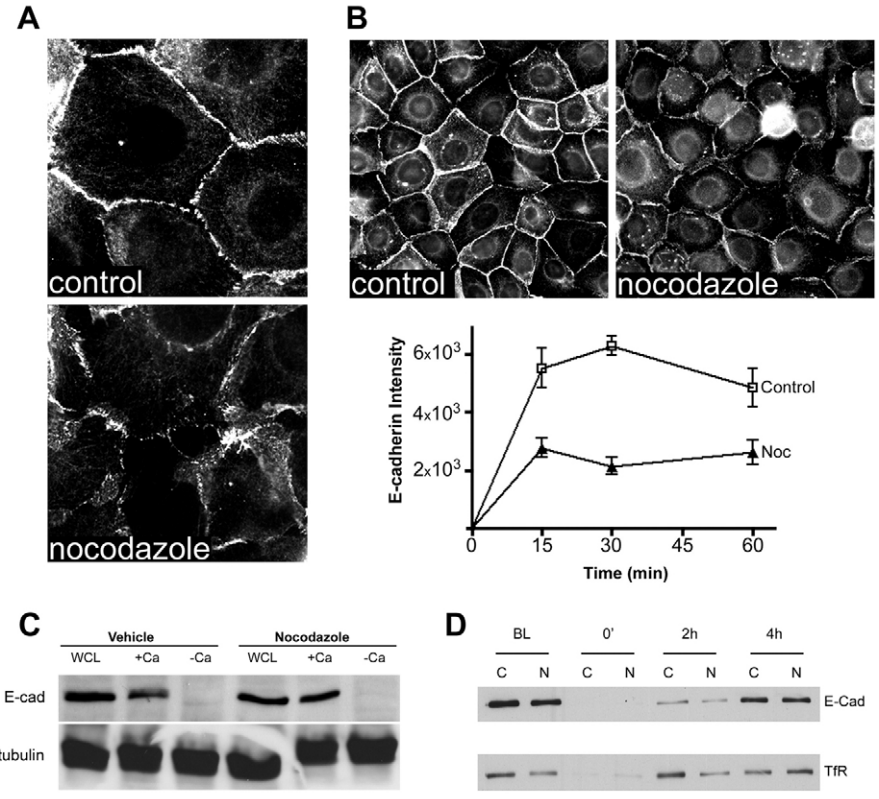

Fig. 5. Nocodazole inhibits the accumulation of E-cadherin at cell-cell contacts without affecting cadherin traffic to the cell surface. (A) Low concentrations of nocodazole disrupt the morphology of cadherin-based cell-cell contacts. MCF-7 monolayers were incubated with nocodazole (100 nM, 240 minutes) or DMSO carrier (Control) before fixation and immunostaining for E-cadherin. (B) Nocodazole reduces E-cadherin accumulation in newly forming cell-cell contacts. Cells were incubated with nocodazole (100 nM, Noc) or DMSO vehicle alone (Control) for 60 minutes beforehand, and throughout the experiments. Cell-cell contacts between confluent MCF-7 cells were disrupted by chelation of extracellular Ca^{2+} (0 minutes) then allowed to reform by addition of Ca^{2+}. At varying times thereafter, samples were fixed and stained for E-cadherin. E-cadherin fluorescence intensity at cell-cell contacts (E-cadherin intensity) was measured by digital image analysis. Representative images of control and nocodazole-treated cells at 30 minutes are shown. (C) Nocodazole does not affect total or surface expression levels of E-cadherin. Surface expression of E-cadherin was measured using surface trypsin protection assays in control cells or cells pre-incubated with nocodazole (100 nM, 90 minutes). Cells were lysed immediately (WCL) or after trypsinisation in the presence (+Ca) or absence (–Ca) of extracellular Ca^{2+}. Total cellular levels of E-cadherin (E-cad) were unaffected by nocodazole and all the cadherin remained accessible to surface trypsinisation in the absence of Ca^{2+} in both the control and drug-treated cells. (D) Nocodazole does not affect transport of E-cadherin to the cell surface. Cells were studied at baseline (BL) or trypsinised to strip E-cadherin from the cell surface (0'), then incubated for 2-4 hours before surface biotinylation. Biotinylated proteins were separated by SDS-PAGE and immunoblotted for E-cadherin or transferrin receptor (TfR), as a loading control. Cultures were incubated in the presence of nocodazole (100 nM, pre-incubated for 1 hour, then for the duration of the experiments) or with vehicle alone (C). Results are representative of three independent experiments.

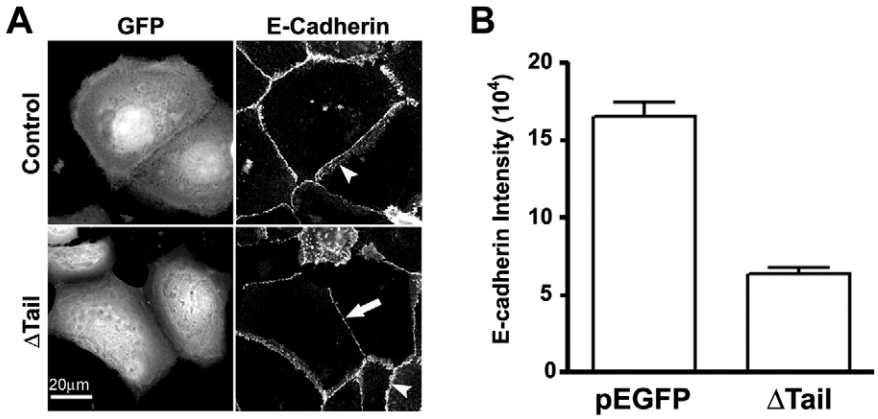

Fig. 6. Mutant CLIP-170 perturbs the focal accumulation of E-cadherin at cell-cell contacts. (A) MCF-7 monolayers were transiently transfected with CLIP-170 Δ-Tail (ΔTail) or with a control vector expressing GFP alone. After 12-24 hours, cells were fixed and immunolabelled for GFP and E-cadherin to identify the transfected cells and cell-cell contacts, respectively. E-cadherin accumulation was reduced at contacts between cells expressing CLIP-170 Δ-Tail (A, arrow) in comparison with contacts between cells that were untransfected or expressing GFP alone (A, arrowhead). (B) Quantitative image analysis was used to measure E-cadherin accumulation at cell-cell contacts between transfected cells, both expressing either CLIP-170 Δ-Tail or GFP alone (pEGFP). Data are means ± s.e.m. (n=60 contacts) and are representative of three separate experiments.

To pursue this notion, we used fluorescence recovery after photobleaching (FRAP) analysis to provide a dynamic index of cadherin accumulation at cell-cell contacts (Fig. 7). The ability of cells to concentrate cadherins at cell-cell contacts is an active process that occurs even in established epithelial monolayers (Adams et al., 1998; Shewan et al., 2005). We reasoned that, under steady-state conditions, changes in the ability of cadherins to concentrate at cell-cell contacts would be reflected by alterations in fluorescence recovery. For these experiments, we used CHO cells stably expressing human E-cadherin bearing a C-terminal YFP tag (hE-YFP-CHO cells (Shewan et al., 2005). Like other GFP-tagged cadherins, this construct was efficiently expressed on the cell surface, accumulated at cell-cell contacts, co-immunoprecipitated catenins and supported cell adhesion (not shown). As we reported recently (Shewan et al., 2005), hE-Cad-YFP fluorescence in contacts between control cells recovers quite rapidly following photobleaching, reaching ~70-80% of baseline within <30 minutes. By contrast, fluorescence recovery was significantly retarded in cells treated with nocodazole (100 nM, 60 minutes; Fig. 7A), with decreases both in the rate of recovery and % recovery (Table 1). Fluorescence recovery was also substantially reduced at contacts between cells expressing CLIP-170 Δ-Tail (Fig. 7B; Table 2), with changes similar to those seen with nocodazole. Taken together, these data indicate that perturbing MT(+)-end dynamics significantly compromises the ability of cells to concentrate cadherins at cell-cell contacts.

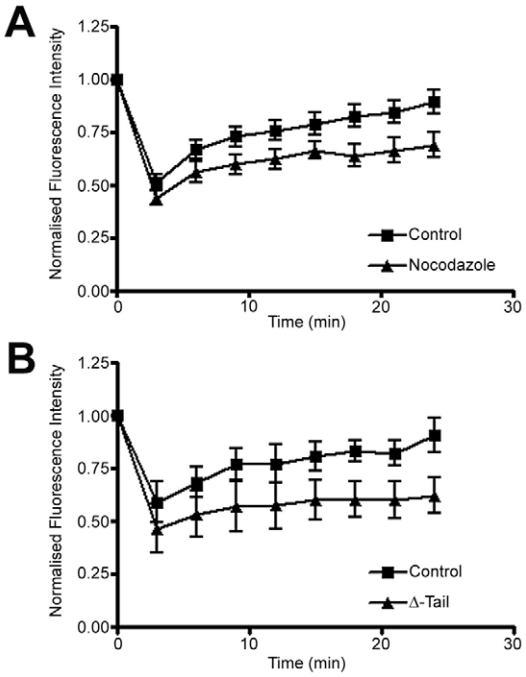

Fig. 7. Recovery of E-cadherin-YFP fluorescence following photobleaching of cell-cell contacts is perturbed by manoeuvres that disrupt dynamic MTs. Cell-cell contacts between CHO cells stably expressing E-Cad-YFP were photobleached and fluorescence recovery imaged by epi-illumination microscopy as described in the Materials and Methods. (A) Cells were incubated with nocodazole (100 nM) or DMSO (Control). (B) Cells were co-microinjected with HA-tagged CLIP-170 Δ-Tail and mRFP for identification (Δ-Tail) or with mRFP alone (Control). Fluorescence intensity at cell-cell contacts following photobleaching was normalised to the fluorescence intensity at the contacts prior to photobleaching as described in the Materials and Methods.

Nocodazole does not affect the trafficking of E-cadherin to the cell surface

One way that MTs might influence cadherin expression at

Table 1. FRAP analysis of E-cadherin dynamic behaviour at contacts between hE-Cad-YFP-CHO cells treated with nocodazole (100 nM)

Treatment	% Recovery	Rate constant of recovery (minutes^{-1})	$t_{1/2}$ (minutes)
Control	89.07±5.63	0.095±0.030	8.261±1.22
Nocodazole (100 mM)	68.84±6.00*	0.039±0.007*	23.88±3.61*

Contacts between CHO cells stably expressing E-Cad-YFP were photobleached, and fluorescence recovery monitored and analysed as described in the Materials and Methods. Data are presented as means ± s.e.m. (n=7). The significance of data was determined by Student's t test, where * indicates P<0.05 compared with controls.

Table 2. FRAP analysis of E-cadherin dynamic behaviour at contacts between hE-Cad-YFP-CHO cells transfected with CLIP-170 Δ-Tail

Treatment	% Recovery	Rate constant of recovery (minutes^{-1})	$t_{1/2}$ (minutes)
Control	90.5±7.80	0.058±0.016	13.20±3.37
CLIP-170 Δ-Tail	61.88±8.30*	0.015±0.010*	60.74±18.43*

Cells stably expressing E-Cad-YFP were microinjected with CLIP-170 Δ-Tail and mRFP (for identification) or with mRFP alone (Control). Contacts between cells transiently expressing the microinjected transgenes were photobleached and fluorescence recovery assayed as described in the Materials and Methods. Data are presented as means ± s.e.m. (n=6). The significance of data was determined by Student's t test, where * indicates P<0.05 compared with controls.

cell-cell contacts is by supporting vesicular transport of cadherins to the cell surface, either through the biosynthetic or recycling pathways (Bryant and Stow, 2004). To examine this possibility, we first assessed the impact of nocodazole on the surface expression of E-cadherin in MCF-7 cells using trypsin protection assays (Fig. 5C). These assays exploit the fact that surface E-cadherin is sensitive to digestion by extracellular trypsin in the absence of Ca^{2+} (Takeichi, 1977): the difference between the total cadherin levels and what remains after trypsinisation in the absence of Ca^{2+} thus provides a reliable index of surface expression (Yap et al., 1997). Nocodazole was used for these experiments as it provided the opportunity to affect whole cell populations for biochemical analysis. We found that both the total and surface levels of E-cadherin were similar in nocodazole-treated cells as in control cells (Fig. 5C). In both cases, the vast majority of E-cadherin was accessible to trypsin digestion in the absence of extracellular Ca^{2+}, and was therefore located on the cell surface.

We then tested whether delivery of cadherins to the cell surface was affected by nocodazole under conditions where this drug clearly perturbed the focal concentration of cadherins. E-cadherin was first stripped from the surfaces of cells by trypsin digestion and the recovery of cadherin at the cell surface monitored by surface biotinylation (Fig. 5D). The initial enzyme treatment effectively removed E-cadherin, as scant E-cadherin was detectable by biotinylation immediately after trypsinisation. Significant recovery of surface E-cadherin was first detected in control cells after ~2 hours recovery and increased by 4 hours. Recovery of cell-surface E-cadherin was not significantly affected by nocodazole. Therefore, changes in vesicular transport of E-cadherin to the cell surface do not readily explain the impact of MT (+)-end dynamics on cadherin accumulation at cell-cell contacts.

Dynamic MTs are necessary for activation of myosin II at cell-cell contacts

The ability of cells to concentrate cadherins at cell-cell contacts is an active process that requires functional cooperation between the adhesive binding of the ectodomain and cytoplasmic determinants, notably myosin II. We recently found that myosin II is recruited to, and activated at, cadherin-based adhesive contacts in response to Rho kinase signalling (Shewan et al., 2005). Importantly, myosin activation was necessary for E-cadherin to accumulate locally at cell-cell contacts. Given the observed impact of nocodazole and mutant

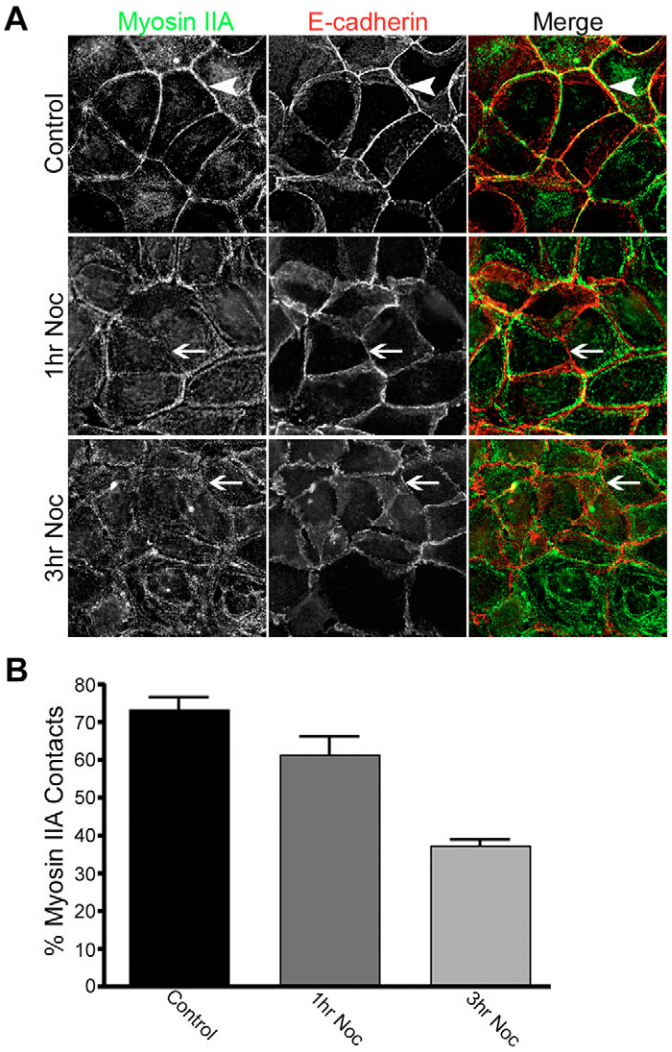

Fig. 8. Dynamic MTs are necessary for accumulation of myosin II at cell-cell contacts. MCF-7 cells were incubated with nocodazole (100 nM) for 1-3 hours, then fixed and stained for myosin IIA and E-cadherin. (A) Myosin IIA and E-cadherin displayed consistent co-localisation in control cells (arrowhead). By contrast, after treatment with nocodazole (Noc), many cadherin-containing contacts showed little myosin IIA staining (arrow). (B) Quantitation of myosin IIA localisation at cadherin-based cell-cell contacts was performed by counting the number of cadherin-positive contacts that also showed co-localised myosin IIA staining. Cell-cell contacts were scored as positive for myosin IIA if they showed clear co-localisation of myosin IIA staining with E-cadherin. All other contacts that failed to show co-localisation of myosin IIA and E-cadherin were scored as negative. Data are means ± s.e.m. (n=150).

CLIP-170 on cadherin accumulation, we hypothesised that dynamic MTs might exert their effects by controlling myosin II activity at cadherin adhesive contacts.

To test this, we first examined the effect of nocodazole on myosin II localisation at contacts between MCF-7 cells (Fig. 8). In control cells, myosin II co-stained with E-cadherin at cell-cell contacts as well as in the immediate peri-junctional area (Fig. 8). By contrast, myosin II staining was reduced at contacts between cells within 1 hour after treatment with

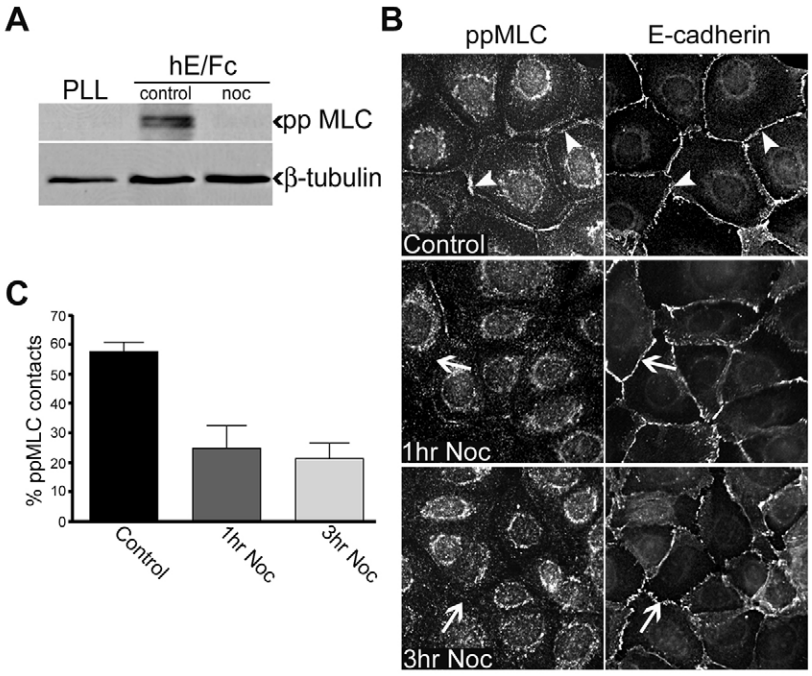

Fig. 9. Dynamic MTs are necessary for myosin II activation at cell-cell contacts. (A) Nocodazole blocks activation of MLC by E-cadherin homophilic ligation. Control MCF-7 cells or cells pretreated with nocodazole (100 nM, 60 minutes; noc) were allowed to adhere to hE/Fc- or poly-L-lysine (PLL)-coated substrata for 90 minutes before lysis. Western blots of cell lysates were probed for activation-specific phosphorylated MLC (ppMLC) or β-tubulin as a loading control. (B,C) Nocodazole blocks accumulation of phosphorylated MLC at cell-cell contacts. Confluent MCF-7 monolayers were incubated with nocodazole (100 nM) for 1-3 hours, then processed and stained for phosphorylated MLC or E-cadherin. (B) Phosphorylated MLC staining was consistently observed at cadherin-based cell-cell contacts in control cells (arrowheads). By contrast, many contacts in nocodazole-treated cells showed little or no co-accumulation of phosphorylated MLC (arrows). (C) Co-accumulation of phosphorylated MLC at cadherin cell-cell contacts was quantitated by counting the number of cadherin-positive contacts that also showed phosphorylated MLC staining.

nocodazole (100 nM). Whereas myosin II co-accumulated with the majority of contacts between control cells, contacts in nocodazole-treated cells often showed little or no co-staining for myosin II, a trend that increased with time (Fig. 8). Myosin II accumulation at cadherin contacts was similarly reduced in cells transiently expressing CLIP-170 Δ-Tail (not shown). These observations thus suggested that dynamic MTs could indeed influence the junctional accumulation of myosin II.

We then asked whether activation of myosin II at cadherin contacts was affected by nocodazole (Fig. 9). Myosin II is activated by phosphorylation of its regulatory myosin light chain (MLC) at Thr18 and Ser19 (Bresnick, 1999), a process that can be assayed using antibodies that specifically detect phosphorylated MLC. As we reported recently (Shewan et al., 2005), adhesion of MCF-7 cells to hE/Fc-coated substrata increased levels of phosphorylated MLC compared with adhesion to poly-L-lysine (PLL)-coated substrata (Fig. 9A), indicating that cadherin homophilic ligation can activate myosin II. Strikingly, treatment with nocodazole (100 nM) largely abolished MLC phosphorylation in response to hE/Fc adhesion, indicating that dynamic MT(+)-ends were necessary for cadherin homophilic adhesion to activate myosin II. Furthermore, whereas phosphorylated MLC could be clearly detected by immunofluorescence microscopy at contacts between control cells, little phosphorylated MLC staining was detected at contacts between either nododazole-treated cells (Fig. 9B,C) or between cells transiently expressing CLIP-170 Δ-Tail (not shown). Consistent with the myosin IIA staining, MLC staining at cell-cell contacts was also reduced in nocodazole-treated cells, without an apparent change in the overall cellular levels of MLC expression (not shown). Together, these findings indicate that dynamic MT(+)-ends are necessary for myosin II activation, both in response to homophilic cadherin adhesion and at native cell-cell contacts in MCF-7 monolayers.

Discussion

Despite important precedents in the literature, the capacity for cadherin adhesions to interact with MTs has been less extensively explored than the well-documented relationship between cadherins and the actin cytoskeleton. In epithelial cells, MTs have been thought principally to run parallel to the contacts, with their (+)-ends oriented towards the basal poles of the cells (Bacallao et al., 1989; Gilbert et al., 1991). In the present studies, we identified a subpopulation of MTs that extended radially into, and appeared to terminate at, sites of E-cadherin adhesion. As such, these radial MTs resembled the MTs reported to orientate towards cell-cell contacts between myoblasts (Mary et al., 2002). Radial MTs were identifiable in a range of epithelial cell lines, as well as in CHO cells stably expressing E-cadherin, whereas ultrastructural studies confirmed that MTs extended into very close proximity with the adherens junctions, consistent with our observation that MT and E-cadherin fluorescence often overlapped at contacts. These MTs were oriented with their (+)-ends directed towards cell-cell contacts, as demonstrated by staining for CLIP-170, which decorated the ends of MTs entering the contacts. Moreover, manoeuvres that perturbed the dynamic integrity of MT(+)-ends significantly reduced the prevalence of radial MTs found at both established cell-cell contacts and contacts that were in the process of reassembly. Together, these data lead us to conclude that, in epithelial cells, a subpopulation of MTs can extend into cadherin-based cell-cell contacts with their (+)-ends oriented towards the adhesive sites.

Importantly, we found that dynamic MTs were crucial for cells to concentrate E-cadherin at cell-cell contacts. Thus, in quantitative immunofluorescence studies, both nocodazole and mutant CLIP-170 perturbed the accumulation of E-cadherin at cell-cell contacts, the intense concentration of cadherin staining typically seen at the apices of contacts between control cells being replaced by staining that was fainter and often discontinuous. Consistent with this, both manoeuvres also

dramatically reduced the ability of E-Cad-YFP fluorescence to recover at cell-cell contacts following photobleaching. Decreased fluorescence recovery could reflect a defect in the ability of cells to replenish cadherin at contacts, implying that dynamic (+)-ends promote the accumulation of cadherins at contacts. Alternatively, fluorescence recovery might be impeded if photobleached cadherin molecules persisted in the contacts, and thereby limited access of fluorescent molecules to cell-cell contacts; this second interpretation would be consistent with the observation that dynamic (+)-ends can destabilise focal adhesions (Small and Kaverina, 2003). However, this scenario predicts that cadherin concentration at cell-cell contacts would persist or increase in cells treated with nocodazole, rather than be reduced as we observed in quantitative immunofluorescence studies. Taken together, these data strongly suggest that dynamic MTs promote E-cadherin accumulation at cell-cell contacts.

One possible explanation for this effect is that MTs support the vesicular transport of cadherin to the cell surface. Cadherin-containing vesicles have been observed to move in a kinesin-dependent fashion along MTs (Mary et al., 2002). However, like others (Adams et al., 1998), we have not observed the movement of hE-Cad-YFP vesicles into contacts in our time-lapse movies (not shown). Importantly, in our studies, nocodazole did not detectably affect the delivery of E-cadherin to the cell surface, as measured by surface biotinylation. Moreover, neither total E-cadherin levels nor cell-surface expression of E-cadherin were affected by nocodazole in our studies. This indicates that the reduced cadherin accumulation at contacts did not reflect changes in the total amount of E-cadherin at the cell surface. Note that we focused on relatively short time spans, but ones where we saw clear changes in cadherin accumulation. Therefore, although we cannot rule out subtle effects or contributions over longer time spans, MT-dependent trafficking of E-cadherin does not adequately explain how dynamic MTs affect the ability of cells to concentrate E-cadherin at contacts. Instead, the loss of cadherin accumulation at the apical regions of cell-cell contacts must reflect the redistribution of cadherin to other areas of the cell surface.

This implies that dynamic MTs are necessary for epithelial cells to accumulate and concentrate E-cadherin at cell-cell contacts once it is on the cell surface. Our findings thus extend the important earlier observation that nocodazole perturbed the integrity of cell contacts (Waterman-Storer et al., 2000), to indicate that this reflects a mechanism by which dynamic MTs regulate the regional distribution of E-cadherin at the plasma membrane. This is consistent with increasing evidence that cadherin adhesion molecules do not distribute passively on the cell surface (Shewan et al., 2005). Instead, classical cadherins concentrate at cell-cell contacts as an active response to homophilic adhesive ligation. This process of local concentration contributes to adhesive strengthening, cell-cell cohesion, and the assembly of adherens and other specialised epithelial junctions. Importantly, such local accumulation requires functional cooperation between the adhesive binding activity of the cadherin ectodomain and cytoplasmic factors. Our current findings thus identify dynamic MTs as one of those cytoplasmic requirements.

How, then, might dynamic MTs control the regional distribution of E-cadherin at the cell surface? One mechanism might involve regulating myosin II activity. We recently reported that myosin II accumulates at cell-cell contacts in response to cadherin adhesion and is crucial for E-cadherin to concentrate at these contacts (Shewan et al., 2005). Indeed, in these studies, inhibition of myosin II activity reduced cadherin accumulation at contacts in a manner very similar to that observed when dynamic MTs were perturbed. Importantly, in our current experiments, we found that blocking dynamic MTs inhibited the ability of E-cadherin to activate and accumulate myosin II at adhesive contacts. We therefore postulate that dynamic MTs promote the local concentration of E-cadherin by regulating myosin II activity at cell-cell contacts. How this regulation is achieved remains to be determined. Possibilities include transport of myosin II to cadherin adhesions, as well as regulation of cell signals that activate myosin II, a notion consistent with emerging evidence that MT(+)-ends can regulate signalling events at cell cortices (Rodriguez et al., 2003). Since myosin II acts as an actin-dependent motor, such a role for dynamic MTs in the regulation of myosin II activity would also be consistent with increasing evidence for a functional interplay between MTs and the actin cytoskeleton, in this case acting at cadherin adhesive contacts (Kodama et al., 2004; Rodriguez et al., 2003).

Finally, our data point to the capacity for cadherin adhesion and MTs to cooperate functionally. Thus, not only do dynamic MTs support the local accumulation of E-cadherin at cell-cell contacts, but we also found that cadherin homophilic adhesion was sufficient to recruit MTs, as demonstrated by the observation that cadherin-coated beads recruited MTs significantly more effectively than ConA-coated beads. This implies that radial MTs could extend into cadherin contacts as a response to cadherin adhesion itself. Such cooperation between E-cadherin and MTs might reflect a multi-phasic process by which cadherin-based cell-cell contacts are assembled and maintained. Even isolated cells display significant complements of surface E-cadherin. Ligation of these free cadherins, when migrating cells make contact with one another or when cells remodel contacts, initiates a cascade of cellular events (Ehrlich et al., 2002) that include, as our current data suggest, the recruitment of dynamic MTs. We postulate that these dynamic MTs then promote the local accumulation of surface E-cadherin at contacts, perhaps through activation of myosin II. The apparently commonplace ability of cells to concentrate cadherins at cell-cell contacts might then reflect a complex interplay between cadherin adhesion, cell signalling and elements of both the MT and actin-based cytoskeletons.

Materials and Methods

Cell culture and purification of hE/Fc

hE-CHO cells and hE-Cad 764AAA-CHO cells were prepared and cultured as described previously (Goodwin et al., 2003; Kovacs et al., 2002a). hE-YFP-CHO cells were described recently (Shewan et al., 2005). MCF-7 cells were cultured in Dulbecco's modified Eagle's medium supplemented with 10% FBS and 2 mM glutamine. Transgenes were expressed by transient transfection using LipofectAMINE^{TM} PLUS or LipofectAMINE^{TM} 2000 (Invitrogen) according to the manufacturer's instructions, or cells were microinjected with 50-100 ng DNA. Purification of hE/Fc and preparation of hE/Fc-coated substrata and latex beads (6 μm-diameter) were performed as described previously (Kovacs et al., 2002b).

Antibodies

Primary antibodies were as follows: (1) mouse monoclonal antibody (mAb) against the cytoplasmic tail of human E-cadherin (Transduction Laboratories); (2) mouse mAb HECD-1 against human E-cadherin (a kind gift from P. Wheelock (Nebraska

Medical Center, Omaha, NE) with the permission of M. Takeichi (RIKEN Center for Developmental Biology, Kobe, Japan); (3) rabbit polyclonal (p)Ab directed against human E-cadherin ectodomain was as previously described (Helwani et al., 2004); (4) rat mAb YOL-1 anti-tubulin (Sera Lab); (5) mouse mAb anti-β-tubulin (Sigma); (6) mouse mAb against acetylated tubulin (clone 6-11B-1; Sigma); (7) rabbit pAb no. 2360, specific for CLIP-170 (Komarova et al., 2002); (8) rabbit pAb for human non-muscle myosin IIA heavy chain (Covance); (9) pAb against phosphorylated MLC (a kind gift from J. Staddon, EISAI, London, UK) (Niggli, 2003); (10) mouse anti-GFP mAb (Roche). F-actin was identified with TRITC-phalloidin (Sigma). Secondary antibodies were species-specific antibodies conjugated with Alexa® Fluor 350, Alexa® Fluor 488, Alexa® Fluor 594 (Molecular Probes), or Cy3 (Jackson Immuno Research Labs).

Plasmids

The GFP and HA-tagged CLIP-170 constructs (Δ tail amino acids 4-309 and wild-type amino acids 4-1320) were described previously (Akhmanova et al., 2001; Komarova et al., 2002).

Immunofluorescence microscopy and image analysis

Specimens were generally fixed in methanol for 5 minutes at –20°C and blocked with 0.5% (w/v) bovine serum albumin in phosphate-buffered saline (PBS) prior to immunostaining. For myosin II staining, samples were briefly extracted with non-ionic detergent prior to fixation. Briefly, cells were transferred to ice for 10 minutes, incubated with pre-permeabilisation buffer [0.5% Triton X-100 in cytoskeleton stabilisation buffer (CSK): 10 mM Pipes pH 6.8, 50 mM NaCl, 3 mM $MgCl_2$, 300 mM sucrose containing 1× complete protease inhibitors (Roche)] for 10 minutes followed by fixation with paraformaldehyde (4% PFA in CSK) for 20 minutes at room temperature. For staining phosphorylated MLC, samples were washed in TBS rather than PBS. Samples were mounted in 50% glycerol, 1% *n*-propyl-gallate in PBS. Images were acquired using an IX81 Olympus Microscope and Hamamatsu Orca-ER camera for epi-illumination or a Zeiss 510 Meta laser-scanning confocal microscope. For some experiments, epi-illumination stacks were deconvolved using the Autoquant system. Single optical slices from both confocal and deconvolved data are shown in the Results. Levels of cadherin accumulation at cell-cell contacts were quantified from epi-illumination images using the line-scan function in MetaMorph (Verma et al., 2004). In brief, contacts were identified and the line-scan function then automatically defined 40 lines oriented perpendicular to the contact, each 120 pixels in length covering a width of 50 pixels. Pixel intensity across each line was measured and processed to generate average values for each corresponding point in the 40 lines, thereby yielding pixel intensity averages across the 120 pixel-long line. The peak pixel intensity value was taken as the measure of fluorescence intensity at the contact. A minimum of 20 contacts were analysed per experiment and experiments were repeated three times.

Live cell imaging

Cells grown on 25 mm round coverslips (size 1, Mediglass, Australia) were imaged in a custom-built heated water jacket maintained at 37.4°C at the coverslip. During imaging, cells were incubated in HBSS without Phenol Red supplemented with 10 mM HEPES (pH 7.4) and 5 mM $CaCl_2$. Epifluorescent live-cell imaging was performed using an Olympus IX81 microscope equipped with 60× and 100× Plan-Apo objectives (NA 1.4) and Hamamatsu Orca1-ER cameras controlled with Metamorph and Olympus IX-2 software. Fluorescence recovery after photobleaching (FRAP) analysis utilising the epi-illumination microscope has been previously reported (Shewan et al., 2005). Briefly, junctions were identified under low light and a pre-bleach image was captured. The most linear contacts were chosen for photobleaching. Immediately afterwards, the iris field diaphragm was then closed to its minimum diameter and the light path cleared of filters, enabling exposure of the selected region of interest (ROI) to maximal light from the mercury burner for no more than 25 seconds. FRAP time-series movies were then commenced, with images captured every 30 seconds for a total of 20-25 minutes. Cells were pre-treated with nocodazole (100 nM) or vector for 60 minutes at 37°C prior to transfer to the heated slide mount and incubated in media containing the appropriate agent for the course of the experiment. FRAP analysis was performed in ImageJ as previously described (Shewan et al., 2005). Briefly, raw data were first adjusted by background subtraction at each time point, corrected to a time-matched ROI in the same sample that had not been photobleached, and then normalised to the background-subtracted pre-bleach image. Kinetic modelling was performed using Prism as recently described (Shewan et al., 2005).

Electron microscopy

Monolayers of MCF-7 cells or hE-CHOs were fixed with 2.5% glutaraldehyde in PBS and then processed for electron microscopy, with 50 nm sections, using standard procedures.

Trypsin protection and surface biotinylation assays

The surface expression of E-cadherin was measured by sensitivity to surface trypsinisation as described previously (Verma et al., 2004). In brief, cells were incubated with crystalline trypsin (0.05% w/v) in Hanks Balanced Salt Solution (HBSS) in the presence of either 2 mM $CaCl_2$ or 5 mM EDTA for 20 minutes at 37°C. Cells were collected and lysed directly into Laemmli sample buffer. Equal volumes of the cellular extracts were separated by SDS-PAGE followed by western analysis with antibodies specific for the ectodomain of E-cadherin (HECD-1) and β-tubulin (as a loading control). Surface biotinylation was performed as previously described (Le et al., 1999). In brief, cells were incubated twice with NHS-Biotin (Pierce; 25 minutes, 4°C, in PBS) and free sulfo-NHS-biotin was quenched with several washes of NH_4Cl (50 mM in PBS). Cells were lysed in RIPA buffer and biotinylated proteins collected with streptavidin beads (Pierce) and processed for western blotting.

We thank our many colleagues who provided generous gifts of plasmids and antibodies, and C. Buttery and T. Munchow for assistance with tissue culture. Above all, we thank our friends and colleagues in the lab for their never-failing support, advice and encouragement. This work was funded by the National Health and Medical Research Council (NHMRC) of Australia and the Human Frontiers Science Program. A.S.Y. was a Wellcome Trust Senior International Medical Research Fellow and R.G.P. a Principal Research Fellow of the NHMRC. A.S.Y. and R.G.P. are Research Affiliates of the ARC Special Research Council for Functional and Applied Genomics, which provided infrastructure support for this work. Confocal microscopy was performed at the ACRF/IMB Dynamic Imaging Centre for Cancer Biology, established with the generous support of the Australian Cancer Research Foundation.

References

Adams, C. L. and Nelson, W. J. (1998). Cytomechanics of cadherin-mediated cell-cell adhesion. *Curr. Opin. Cell Biol.* **10**, 572-577.

Adams, C. L., Chen, Y.-T., Smith, S. J. and Nelson, W. J. (1998). Mechanisms of epithelial cell-cell adhesion and cell compaction revealed by high-resolution tracking of E-cadherin-green fluorescent protein. *J. Cell Biol.* **142**, 1105-1119.

Akhmanova, A. and Hoogenraad, C. C. (2005). Microtubule plus-end-tracking proteins: mechanisms and functions. *Curr. Opin. Cell Biol.* **17**, 47-54.

Akhmanova, A., Hoogenraad, C. C., Drabek, K., Stepanova, T., Dortland, B., Verkerk, T., Vermeulen, W., Burgering, B. M., De Zeeuw, C. I., Grosveld, F. et al. (2001). Clasps are CLIP-115 and –170 associating proteins involved in the regional regulation of microtubule dynamics in motile fibroblasts. *Cell* **104**, 923-935.

Bacallao, R., Antony, C., Karsenti, E., Stelzer, E. and Simons, K. (1989). The subcellular organization of Madin-Darby canine kidney cells during the formation of a polarized epithelium. *J. Cell Biol.* **109**, 2817-2832.

Bresnick, A. R. (1999). Molecular mechanisms of nonmuscle myosin-II regulation. *Curr. Opin. Cell Biol.* **11**, 26-33.

Bryant, D. M. and Stow, J. L. (2004). The ins and outs of E-cadherin trafficking. *Trends Cell Biol.* **14**, 427-434.

Chausovsky, A., Bershadsky, A. D. and Borisy, G. G. (2000). Cadherin-mediated regulation of microtubule dynamics. *Nat. Cell Biol.* **2**, 797-804.

Chen, X., Kojima, S., Borisy, G. G. and Green, K. J. (2003). p120 catenin associates with kinesin and facilitates the transport of cadherin-catenin complexes to intercellular junctions. *J. Cell Biol.* **163**, 547-557.

Ehrlich, J. S., Hansen, M. D. H. and Nelson, W. J. (2002). Spatio-temporal regulation of Rac1 localization and lamelliodia dynamics during epithelial cell-cell adhesion. *Dev. Cell* **3**, 259-270.

Franz, C. M. and Ridley, A. J. (2004). p120 catenin associates with microtubules. Inverse relationship between microtubule binding and Rho GTPase regulation. *J. Biol. Chem.* **279**, 6588-6594.

Gavard, J., Lambert, M., Grosheva, I., Marthiens, V., Irinopoulou, T., Riou, J.-F., Bershadsky, A. and Mege, R. M. (2004). Lamellipodium extension and cadherin adhesion: two cell responses to cadherin activation relying on distinct signalling pathways. *J. Cell Sci.* **117**, 257-270.

Gilbert, T., Le Bivic, A., Quaroni, A. and Rodriguez-Boulan, E. (1991). Microtubular organization and its involvement in the biogenetic pathways of plasma membrane proteins in Caco-2 intestinal epithelial cells. *J. Cell Biol.* **113**, 275-288.

Goodwin, M., Kovacs, E. M., Thoreson, M. A., Reynolds, A. B. and Yap, A. S. (2003). Minimal mutation of the cytoplasmic tail inhibits the ability of E-cadherin to activate Rac but not phosphatidylinositol 3-kinase: direct evidence of a role for cadherin-activated Rac signaling in adhesion and contact formation. *J. Biol. Chem.* **278**, 20533-20539.

Gumbiner, B. M. (2000). Regulation of cadherin adhesive activity. *J. Cell Biol.* **148**, 399-403.

Gundersen, G. G., Gomes, E. R. and Wen, Y. (2004). Cortical control of microtubule stability and polarization. *Curr. Opin. Cell Biol.* **16**, 106-112.

Helwani, F. M., Kovacs, E. M., Paterson, A. D., Verma, S., Ali, R. G., Fanning, A. S., Weed, S. A. and Yap, A. S. (2004). Cortactin is necessary for E-cadherin-mediated contact formation and actin reorganization. *J. Cell Biol.* **164**, 899-910.

Howard, J. and Hyman, A. A. (2003). Dynamics and mechanics of the microtubule plus end. *Nature* **422**, 753-758.

Jordan, M. A. and Wilson, L. (1998). Use of drugs to study role of microtubule assembly dynamics in living cells. *Methods Enzymol.* **298**, 252-276.

Kaufmann, U., Kirsch, J., Irintchev, A., Wernig, A. and Starzinski-Powitz, A. (1999). The M-cadherin catenin complex interacts with microtubules in skeletal muscle cells: implications for the fusion of myoblasts. *J. Cell Sci.* **112**, 55-68.

Kodama, A., Lechler, T. and Fuchs, E. (2004). Coordinating cytoskeletal tracks to polarize cellular movements. *J. Cell Biol.* **167**, 203-207.

Komarova, Y. A., Akhmanova, A. S., Kojima, S., Galjart, N. and Borisy, G. G. (2002). Cytoplasmic linker proteins promote microtubule rescue in vivo. *J. Cell Biol.* **159**, 589-599.

Kovacs, E. M., Ali, R. G., McCormack, A. J. and Yap, A. S. (2002a). E-cadherin homophilic ligation directly signals through Rac and PI3-kinase to regulate adhesive contacts. *J. Biol. Chem.* **277**, 6708-6718.

Kovacs, E. M., Goodwin, M., Ali, R. G., Paterson, A. D. and Yap, A. S. (2002b). Cadherin-directed actin assembly: E-cadherin physically associates with the Arp2/3 complex to direct actin assembly in nascent adhesive contacts. *Curr. Biol.* **12**, 379-382.

Le, T. L., Yap, A. S. and Stow, J. L. (1999). Recycling of E-cadherin: a potential mechanism for regulating cadherin dynamics. *J. Cell Biol.* **146**, 219-232.

Ligon, L. A., Karki, S., Tokito, M. and Holzbaur, E. L. (2001). Dynein binds to beta-catenin and may tether microtubules at adherens junctions. *Nat. Cell Biol.* **3**, 913-917.

Ligon, L. A., Shelly, S. S., Tokito, M. and Holzbaur, E. L. (2003). The microtubule plus-end proteins EB1 and dynactin have differential effects on microtubule polymerization. *Mol. Biol. Cell* **14**, 1405-1417.

Mary, S., Charrasse, S., Meriane, M., Comunale, F., Travo, P., Blangy, A. and Gauthier-Rouviere, C. (2002). Biogenesis of N-Cadherin-dependent cell-cell contacts in living fibroblasts is a microtubule-dependent kinesin-driven mechanism. *Mol. Biol. Cell* **13**, 285-301.

Niggli, V. (2003). Microtubule-disruption-induced and chemotactic-peptide-induced migration of human neutrophils: implications for differential sets of signalling pathways. *J. Cell Sci.* **116**, 813-822.

Perez, F., Diamantopoulos, G. S., Stalder, R. and Kreis, T. E. (1999). CLIP-170 highlights growing microtubule ends in vivo. *Cell* **96**, 517-527.

Perez-Moreno, M., Jamora, C. and Fuchs, E. (2003). Sticky business: orchestrating cellular signals at adherens junctions. *Cell* **112**, 535-548.

Rodriguez, O. C., Schaefer, A. W., Mandato, C. A., Forscher, P., Bement, W. M. and Waterman-Storer, C. M. (2003). Conserved microtubule-actin interactions in cell movement and morphogenesis. *Nat. Cell Biol.* **5**, 599-609.

Shewan, A. M., Maddugoda, M., Kraemer, A., Stehbens, S. J., Verma, S., Kovacs, E. M. and Yap, A. S. (2005). Myosin 2 is a key Rho kinase target necessary for the local concentration of E-cadherin at cell-cell contacts. *Mol. Biol. Cell* **16**, 4531-4532.

Small, J. V. and Kaverina, I. (2003). Microtubules meet substrate adhesions to arrange cell polarity. *Curr. Opin. Cell Biol.* **15**, 40-47.

Takeichi, M. (1977). Functional correlation between cell adhesive properties and some cell surface proteins. *J. Cell Biol.* **75**, 464-474.

Teng, J., Rai, T., Tanaka, Y., Takei, Y., Nakata, T., Hirasawa, M., Kulkarni, A. B. and Hirokawa, N. (2005). The KIF3 motor transports N-cadherin and organizes the developing neuroepithelium. *Nat. Cell Biol.* **7**, 474-482.

Thoreson, M. A., Anastasiadis, P. Z., Daniel, J. M., Ireton, R. C., Wheelock, M. J., Johnson, K. R., Hummingbird, D. K. and Reynolds, A. B. (2000). Selective uncoupling of $p120^{ctn}$ from E-cadherin disrupts strong adhesion. *J. Cell Biol.* **148**, 189-201.

Verma, S., Shewan, A. M., Scott, J. A., Helwani, F. M., Elzen, N. R., Miki, H., Takenawa, T. and Yap, A. S. (2004). Arp2/3 Activity Is Necessary for Efficient Formation of E-cadherin Adhesive Contacts. *J. Biol. Chem.* **279**, 34062-34070.

Watanabe, T., Noritake, J. and Kaibuchi, K. (2005). Regulation of microtubules in cell migration. *Trends Cell Biol.* **15**, 76-83.

Waterman-Storer, C. M., Salmon, W. C. and Salmon, E. D. (2000). Feedback interactions between cell-cell adherens junctions and cytoskeletal dynamics in newt lung epithelial cells. *Mol. Biol. Cell* **11**, 2471-2483.

Yanagisawa, M., Kaverina, I. N., Wang, A., Fujita, Y., Reynolds, A. B. and Anastasiadis, P. Z. (2004). A novel interaction between kinesin and p120 modulates p120 localization and function. *J. Biol. Chem.* **279**, 9512-9521.

Yap, A. S. and Kovacs, E. M. (2003). Direct cadherin-activated cell signaling: a view from the plasma membrane. *J. Cell Biol.* **160**, 11-16.

Yap, A. S., Stevenson, B. R., Abel, K. C., Cragoe, E. J., Jr and Manley, S. W. (1995). Microtubule integrity is necessary for the barrier function of cultured thyroid cell monolayers. *Exp. Cell Res.* **218**, 540-550.

Yap, A. S., Brieher, W. M., Pruschy, M. and Gumbiner, B. M. (1997). Lateral clustering of the adhesive ectodomain: a fundamental determinant of cadherin function. *Curr. Biol.* **7**, 308-315.

Journal of Cell Science